Supporting Information for

Air-stable chiral mono- and dinuclear dysprosium single-molecule magnets: steric hindrance of hexaazamacrocycles

Chen Zhao,[a, b] Zhenhua Zhu,*[a, c] Xiao-Lei Li,[a] and Jinkui Tang[a, b]

[a] State Key Laboratory of Rare Earth Resource Utilization, Changchun Institute of Applied Chemistry, Chinese Academy of Sciences, Changchun 130022, P. R. China.
[b] School of Applied Chemistry and Engineering, University of Science and Technology of China, Hefei 230026, P. R. China.
[c] University of Chinese Academy of Sciences, Beijing 100049, P. R. China.
* Corresponding author

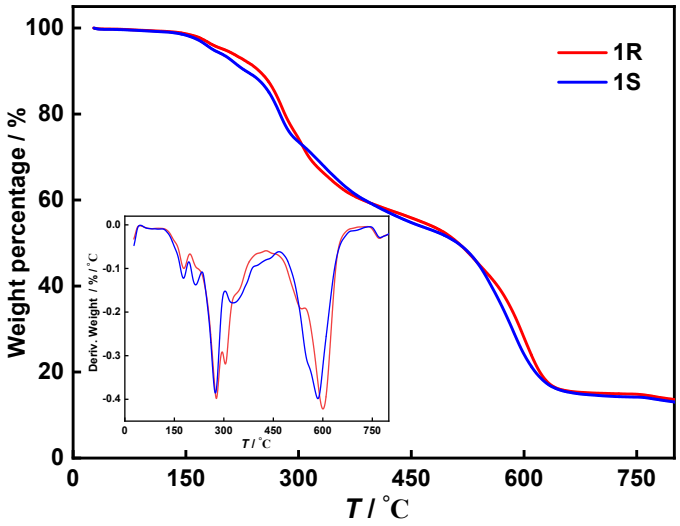

Figure S1. Thermogravimetric analyses of **1R** (red) and **1S** (blue).

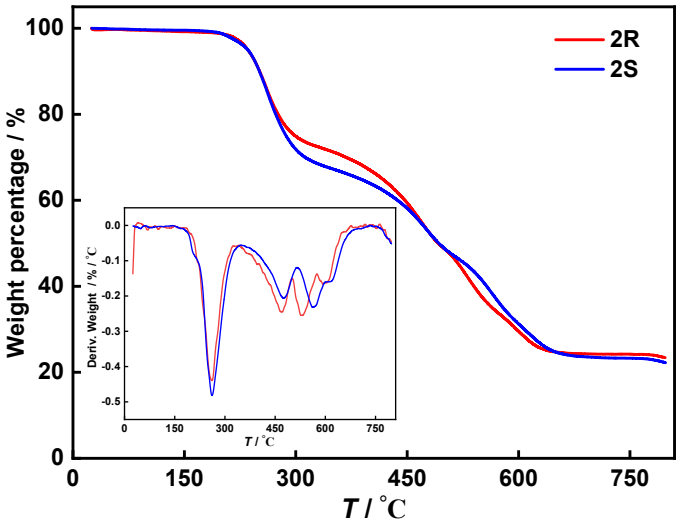

Figure S2. Thermogravimetric analyses of **2R** (red) and **2S** (blue).

Table S1. Crystal Data and Structure Refinement for **1R** and **1S**.

Compound reference	**1R**	**1S**
Chemical formula	$C_{80}H_{68}BDyN_6O_2$	$C_{80}H_{68}BDyN_6O_2$
Formula Mass	1318.71	1318.71
Temperature (K)	180.0	180.0
Crystal system	orthorhombic	orthorhombic
Space group	$P2_12_12_1$	$P2_12_12_1$
a (Å)	15.3455(2)	15.3363(3)
b (Å)	16.8624(3)	16.8363(4)
c (Å)	30.5926(5)	30.5645(5)
α (°)	90	90
β (°)	90	90
γ (°)	90	90
Unit cell volume (Å^3)	7908.4(2)	7892.0(3)
Z	4	4
ρ_{calc} (g/cm^3)	1.108	1.110
μ / mm^{-1}	0.989	0.991
F (000)	2708.0	2708.0
Radiation	MoKα (λ = 0.71073)	MoKα (λ = 0.71073)
Reflections collected	58068	58209
Independent reflections	13856	13819
R_{int}	0.0236	0.0281
GOF on F^2	1.060	1.034
R_1 ($I \geqslant 2\sigma$ (I))	0.0327	0.0310
wR_2 (all data)	0.0962	0.0876
Flack parameter	0.032(3)	0.027(3)
CCDC number	2099516	2099517

Table S2. Crystal Data and Structure Refinement for **2R** and **2S**.

Compound reference	**2R**	**2S**
Chemical formula	$C_{114}H_{116}B_2Dy_2N_{12}O_4$	$C_{114}H_{116}B_2Dy_2N_{12}O_4$
Formula Mass	2064.80	2064.80
Temperature (K)	180.0	180.0
Crystal system	monoclinic	monoclinic
Space group	*C*2	*C*2
a (Å)	24.4235(7)	24.4551(7)
b (Å)	16.4538(5)	16.4773(6)
c (Å)	25.1367(7)	25.1381(8)
α (°)	90	90
β (°)	103.2100(10)	103.3770(10)
γ (°)	90	90
Unit cell volume (Å^3)	9834.1(5)	9854.7(6)
Z	4	4
ρ_{calc} (g/cm^3)	1.395	1.392
μ / mm^{-1}	1.568	1.565
F (000)	4232.0	4232.0
Radiation	MoKα (λ = 0.71073)	MoKα (λ = 0.71073)
Reflections collected	50009	62940
Independent reflections	17293	17368
R_{int}	0.0296	0.0407
GOF on F^2	1.044	1.067
R_1 ($I \geqslant 2\sigma$ (I))	0.0404	0.0510
wR_2 (all data)	0.1089	0.1461
Flack parameter	0.002(5)	0.006(6)
CCDC number	2078250	2078251

Table S3. Selected bond distances (Å) for complexes **1R** and **1S**.

1R		**1S**	
Dy1-O1	2.145(4)	Dy1-O1	2.149(4)
Dy1-O2	2.136(4)	Dy1-O2	2.129(4)
Dy1-N1	2.622(5)	Dy1-N1	2.623(4)
Dy1-N2	2.637(4)	Dy1-N2	2.635(4)
Dy1-N3	2.656(4)	Dy1-N3	2.671(4)
Dy1-N4	2.691(5)	Dy1-N4	2.646(4)
Dy1-N5	2.647(5)	Dy1-N5	2.655(4)
Dy1-N6	2.632(4)	Dy1-N6	2.662(5)

Table S4. Selected bond distances (Å) for complexes **2R** and **2S**.

2R		**2S**	
Dy1-O1	2.138(6)	Dy1-O4	2.2841(5)
Dy1-O2	2.2934(4)	Dy1-O5	2.152(7)
Dy1-O3	2.2825(4)	Dy1-O3	2.2967(5)
Dy1-N1	2.696(8)	Dy1-N7	2.649(11)
Dy1-N2	2.626(7)	Dy1-N8	2.617(9)
Dy1-N3	2.656(8)	Dy1-N9	2.683(10)
Dy1-N4	2.769(8)	Dy1-N10	2.619(9)
Dy1-N5	2.635(7)	Dy1-N11	2.625(9)
Dy1-N6	2.628(8)	Dy1-N12	2.76011)
Dy2-O4	2.131(8)	Dy2-O1	2.2808(6)
Dy2-O5	2.2835(4)	Dy2-O2	2.135(12)
Dy2-O5[1]	2.2819(4)	Dy2-O1[2]	2.2897(6)
Dy2-N7	2.611(11)	Dy2-N1	2.616(14)
Dy2-N8	2.750(9)	Dy2-N2	2.625(9)
Dy2-N9	2.635(12)	Dy2-N3	2.753(13)
Dy2-N10	2.6604(10)	Dy2-N4	2.601(14)
Dy2-N11	2.745(9)	Dy2-N5	2.686(13)
Dy2-N12	2.687(10)	Dy2-N6	2.749(12)

[1]2-X, +Y, -Z; [2]1-X, +Y, -Z

Table S5. Selected bond angles (°) for complexes **1R** and **1S**.

1R		**1S**	
O1-Dy1-O2	170.45(17)	O1-Dy1-O2	170.05(16)
O1-Dy1-N1	85.59(16)	O1-Dy1-N1	85.82(15)
O1-Dy1-N2	82.70(15)	O1-Dy1-N2	82.88(14)
O1-Dy1-N3	87.22(16)	O1-Dy1-N3	87.61(15)
O1-Dy1-N4	81.59(16)	O1-Dy1-N4	92.19(15)
O1-Dy1-N5	103.09(16)	O1-Dy1-N5	103.40(15)
O1-Dy1-N6	92.55(16)	O1-Dy1-N6	81.25(15)
O2-Dy1-N1	98.57(17)	O2-Dy1-N1	98.44(16)
O2-Dy1-N2	93.13(16)	O2-Dy1-N2	92.79(14)
O2-Dy1-N3	98.31(17)	O2-Dy1-N3	98.21(16)
O2-Dy1-N4	92.84(17)	O2-Dy1-N4	77.90(15)
O2-Dy1-N5	86.42(16)	O2-Dy1-N5	86.50(15)
O2-Dy1-N6	77.94(17)	O2-Dy1-N6	92.99(16)
N1-Dy1-N2	168.26(15)	N1-Dy1-N2	168.69(14)
N1-Dy1-N3	117.67(14)	N1-Dy1-N3	117.76(13)
N1-Dy1-N4	61.12(14)	N1-Dy1-N4	120.88(14)
N1-Dy1-N5	61.02(14)	N1-Dy1-N5	60.91(13)
N1-Dy1-N6	121.15(15)	N1-Dy1-N6	60.47(13)
N2-Dy1-N3	61.06(13)	N2-Dy1-N3	61.36(12)
N2-Dy1-N4	117.55(14)	N2-Dy1-N4	60.29(13)
N2-Dy1-N5	121.11(14)	N2-Dy1-N5	121.46(13)
N2-Dy1-N6	60.41(14)	N2-Dy1-N6	117.91(13)
N3-Dy1-N4	168.80(15)	N3-Dy1-N4	121.17(13)
N3-Dy1-N5	60.80(14)	N3-Dy1-N5	60.89(13)
N3-Dy1-N6	120.98(14)	N3-Dy1-N6	168.80(14)
N4-Dy1-N5	121.29(14)	N4-Dy1-N5	164.40(15)
N4-Dy1-N6	60.45(14)	N4-Dy1-N6	60.86(13)
N5-Dy1-N6	164.36(15)	N5-Dy1-N6	120.58(13)

Table S6. Selected bond angles (°) for complexes **2R** and **2S**.

2R		**2S**	
Dy1-O2-Dy1[1]	113.051(17)	Dy1-O3-Dy1[1]	112.91(2)
Dy1-O3-Dy1[1]	113.884(17)	Dy1-O4-Dy1[3]	113.872(2)
Dy2-O5-Dy2[2]	113.749(12)	Dy2-O1-Dy2[4]	113.710(16)
O1-Dy1-O2	145.7(3)	O5-Dy1-O3	145.6(3)
O1-Dy1-O3	147.7(3)	O5-Dy1-O4	147.7(3)
O4-Dy2-O5	145.76(19)	O2-Dy2-O1	147.7(3)
O4-Dy2-O5[2]	147.96(19)	O2-Dy2-O1[4]	146.0(3)
O1-Dy1-N1	79.9(3)	O5-Dy1-N7	78.0(4)
O1-Dy1-N2	94.5(2)	O5-Dy1-N8	94.5(3)
O1-Dy1-N3	78.1(3)	O5-Dy1-N9	79.6(4)
O1-Dy1-N4	78.2(3)	O5-Dy1-N10	76.7(4)
O1-Dy1-N5	93.5(2)	O5-Dy1-N11	93.8(3)
O1-Dy1-N6	76.5(3)	O5-Dy1-N12	78.5(4)
O4-Dy2-N7	93.0(4)	O2-Dy2-N1	94.3(5)
O4-Dy2-N8	78.4(3)	O2-Dy2-N2	77.4(4)
O4-Dy2-N9	77.6(4)	O2-Dy2-N3	78.4(4)
O4-Dy2-N10	94.4(4)	O2-Dy2-N4	93.0(5)
O4-Dy2-N11	79.6(3)	O2-Dy2-N5	76.6(4)
O4-Dy2-N12	76.7(3)	O2-Dy2-N6	79.6(4)
N1-Dy1-N2	60.6(2)	N1-Dy2-N2	62.1(4)
N2-Dy1-N3	60.9(2)	N2-Dy2-N3	61.3(5)
N3-Dy1-N4	60.3(2)	N3-Dy2-N4	59.8(5)
N4-Dy1-N5	59.9(2)	N4-Dy2-N5	60.9(4)
N5-Dy1-N6	61.7(2)	N5-Dy2-N6	59.3(4)
N6-Dy1-N1	61.0(2)	N6-Dy2-N1	60.4(4)
N7-Dy2-N8	59.6(3)	N7-Dy1-N8	60.9(3)
N8-Dy2-N9	61.4(4)	N8-Dy1-N9	60.6(3)
N9-Dy2-N10	62.0(4)	N9-Dy1-N10	61.1(3)
N10-Dy2-N11	60.4(3)	N10-Dy1-N11	61.6(3)
N11-Dy2-N12	59.8(3)	N11-Dy1-N12	59.9(3)
N12-Dy2-N7	60.6(3)	N12-Dy1-N7	60.2(3)

[1]2-X, +Y, 1-Z; [2]2-X, +Y, -Z; [3]1-X, +Y, -Z; [4]1-X, +Y, 1-Z

Table S7. The CShM values calculated by SHAPE 2.1 for **1R** and **2R**.[1, 2]

Central atom	Coordination Geometry	**1R**	**1S**
Dy	Octagon (D_{8h})	31.332	31.270
	Heptagonal pyramid (C_{7v})	21.137	20.983
	Hexagonal bipyramid (D_{6h})	1.860	1.858
	Cube (O_h)	10.189	10.198
	Square antiprism (D_{4d})	16.094	16.117
	Triangular dodecahedron (D_{2d})	13.426	13.407
	Johnson gyrobifastigium J26 (D_{2d})	6.568	6.590
	Johnson elongated triangular bipyramid J14 (D_{3h})	23.392	23.461
	Biaugmented trigonal prism J50 (C_{2v})	14.540	14.550
	Biaugmented trigonal prism (C_{2v})	14.195	14.156
	Snub diphenoid J84 (D_{2d})	14.967	15.013
	Triakis tetrahedron (T_d)	10.999	10.977
	Elongated trigonal bipyramid (D_{3h})	20.999	21.000

Table S8. The CShM values calculated by SHAPE 2.1 for **2R** and **2S**.[1, 2]

Coordination Geometry	**2R**		**2S**	
	Dy1	**Dy2**	**Dy1**	**Dy2**
Enneagon (D_{9h})	32.298	32.244	32.242	32.179
Octagonal pyramid (C_{8v})	22.067	22.002	22.016	22.105
Heptagonal bipyramid (D_{7h})	15.106	14.517	15.053	14.599
Johnson triangular cupola J3 (C_{3v})	14.438	14.559	14.485	14.541
Capped cube J8 (C_{4v})	7.516	7.641	7.529	7.617
Spherical-relaxed capped cube (C_{4v})	6.764	7.010	6.743	7.001
Capped square antiprism J10 (C_{4v})	8.304	8.310	8.244	8.329
Spherical capped square antiprism (C_{4v})	7.375	7.291	7.316	7.297
Tricapped trigonal prism J51 (D_{3h})	7.709	7.627	7.671	7.633
Spherical tricapped trigonal prism (D_{3h})	8.458	8.403	8.382	8.403
Tridiminished icosahedron J63 (C_{3v})	9.352	9.705	9.373	9.645
Hula-hoop (C_{2v})	2.561	2.736	2.512	2.749
Muffin (C_s)	5.654	5.580	5.591	5.578

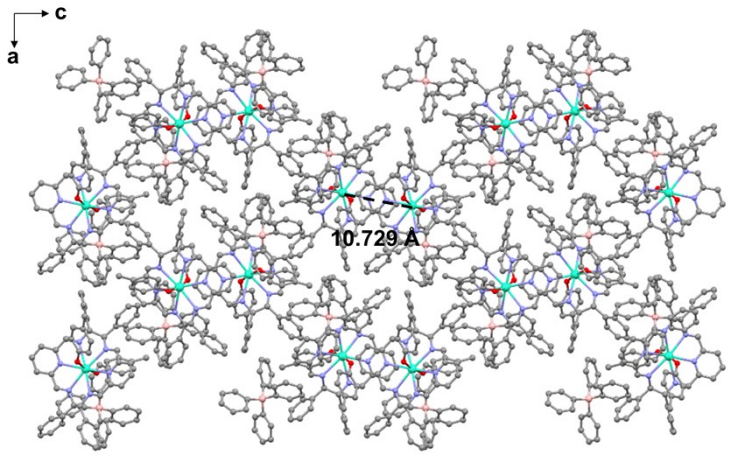

Figure S3. The packing diagram for **1R** shown along the crystallographic *b* axis gives the shortest intermolecular Dy···Dy distance of 10.729 Å.

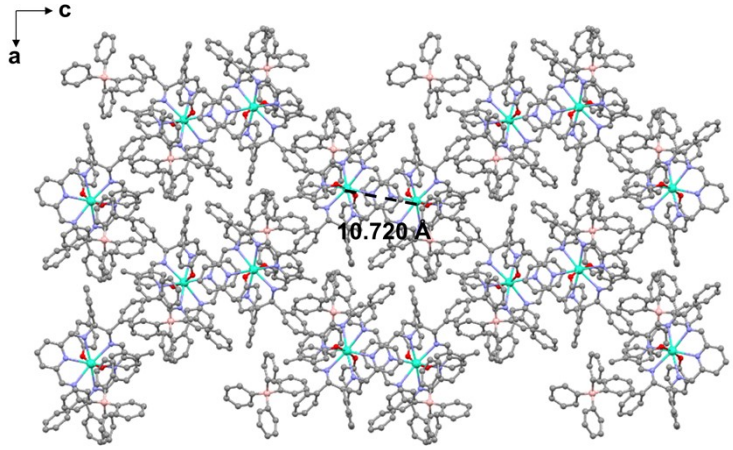

Figure S4. The packing diagram for **1S** shown along the crystallographic *b* axis gives the shortest intermolecular Dy···Dy distance of 10.720 Å.

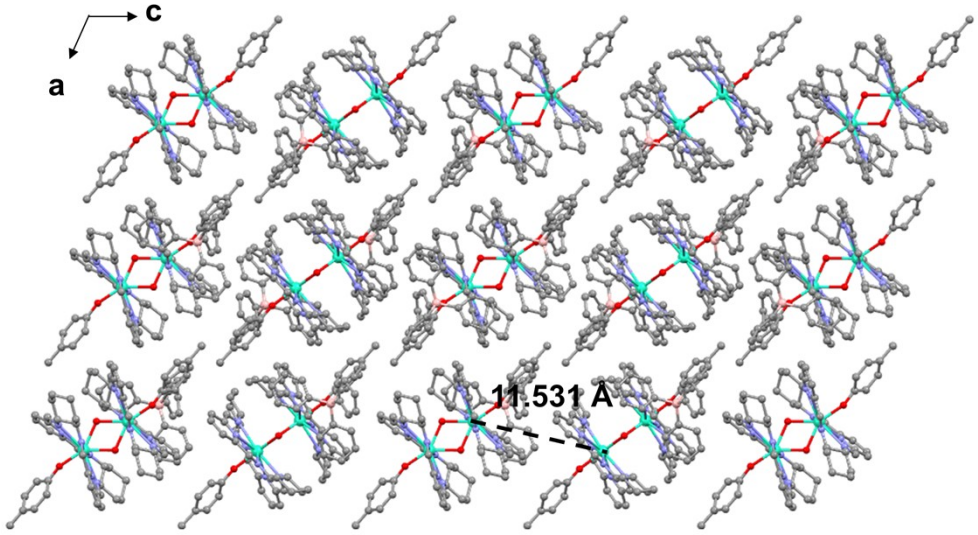

Figure S5. The packing diagram for **2R** shown along the crystallographic *b* axis gives the shortest intermolecular Dy···Dy distance of 11.531 Å.

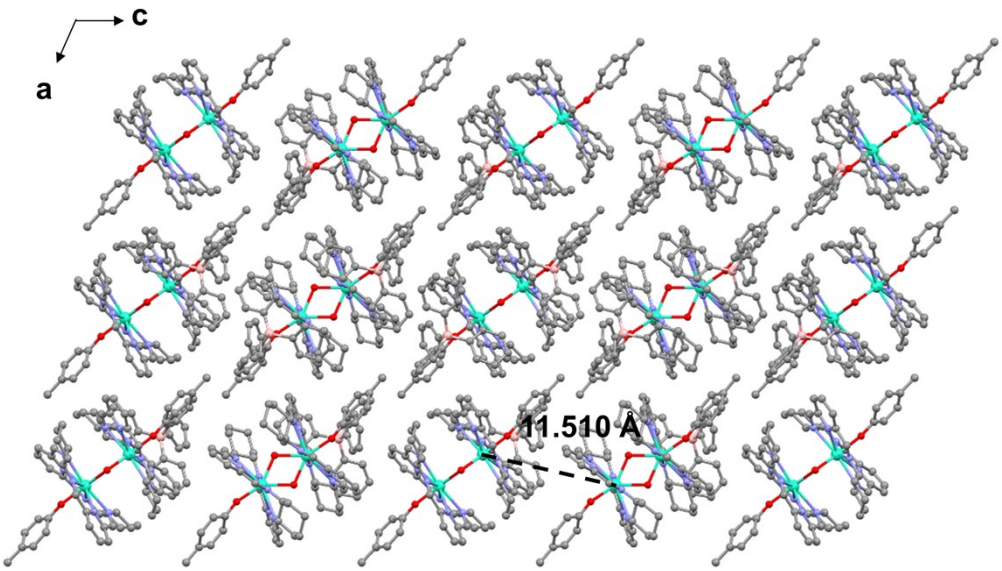

Figure S6. The packing diagram for **2S** shown along the crystallographic *b* axis gives the shortest intermolecular Dy···Dy distance of 11.510 Å.

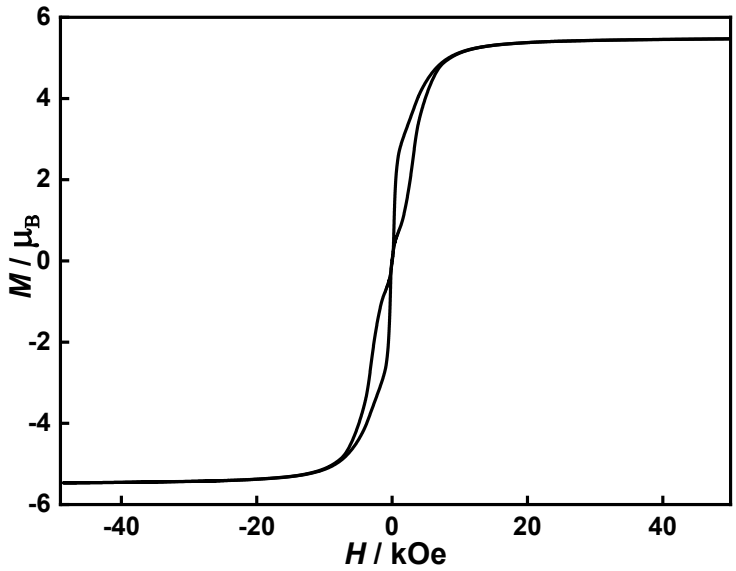

Figure S7. Magnetic hysteresis loop for **1R**. The data were collected at 1.9 K using an average field sweep speed of 31 Oe s^{-1}.

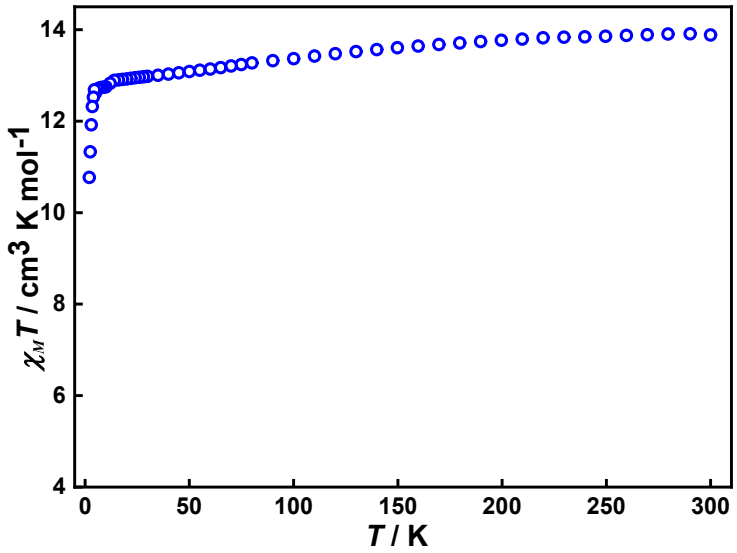

Figure S8. Plots of $\chi_M T$ versus temperature for **1S** in an applied magnetic field of 1 kOe. $\chi_M T$ (300 K) = 13.88 cm^3 K mol^{-1}, $\chi_M T$ (2 K) = 10.77 cm^3 K mol^{-1}.

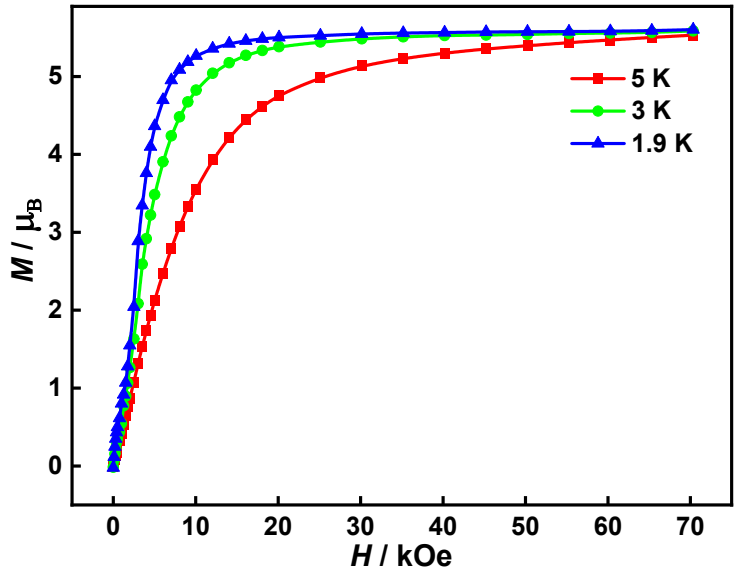

Figure S9. Field dependence of the magnetization at 1.9 K, 3 K and 5 K for **1S**. M = 5.60 μ_B at 1.9 K and 70 kOe.

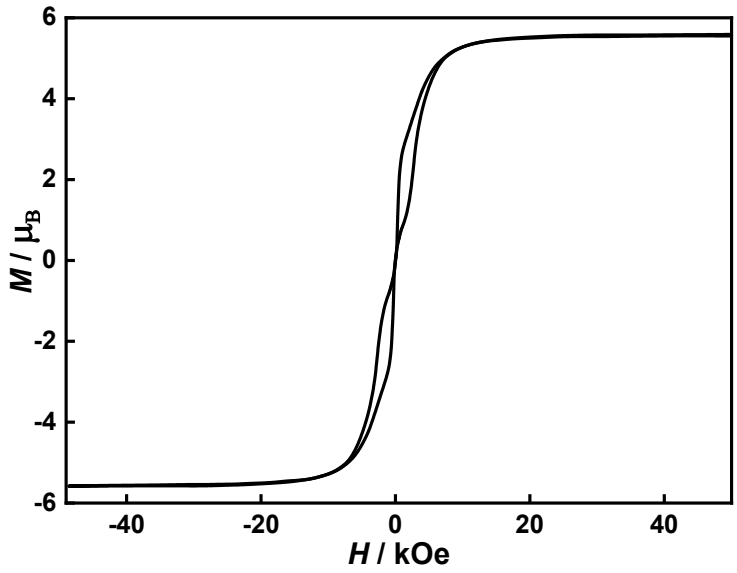

Figure S10. Magnetic hysteresis loop for **1S**. The data were collected at 1.9 K using an average field sweep speed of 31 Oe s^{-1}.

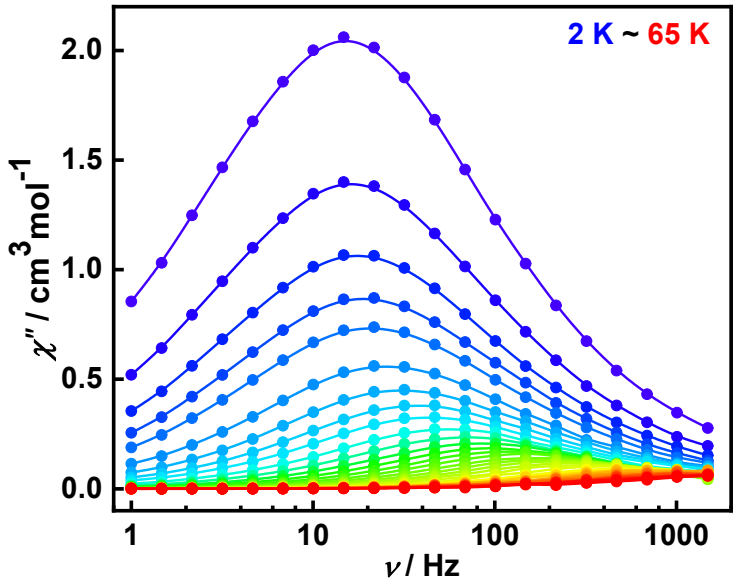

Figure S11. Frequency dependence of the out-of-phase susceptibility (χ'') for **1S** in zero DC field at AC frequencies of 1-1488 Hz in the temperature range of 2 to 65 K.

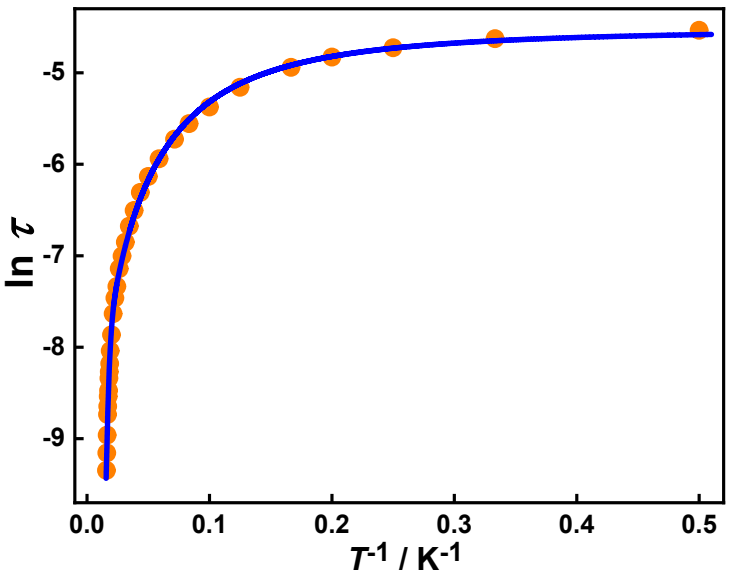

Figure S12. Temperature dependence of the relaxation time in the form of natural logarithm for **1S**. The blue line represents the fitting. The fitting equation is $\ln(\tau) = -\ln[CT^n+\tau_0^{-1}\exp(-U_{eff}/k_BT)+1/\tau_{QTM}]$, giving U_{eff} = 533(11) cm^{-1}, τ_0 = 6.8(3) × 10^{-10} s, C = 1.9(2) s^{-1} K^{-n}, n = 1.78(4), τ_{QTM} = 1.09(4) × 10^{-2} s.

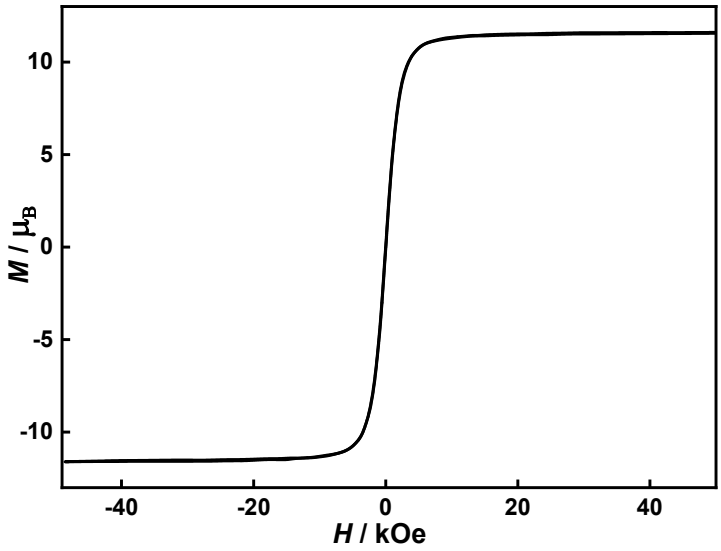

Figure S13. Magnetic hysteresis loop for **2R**. The data were collected at 1.9 K using an average field sweep speed of 31 Oe s^{-1}.

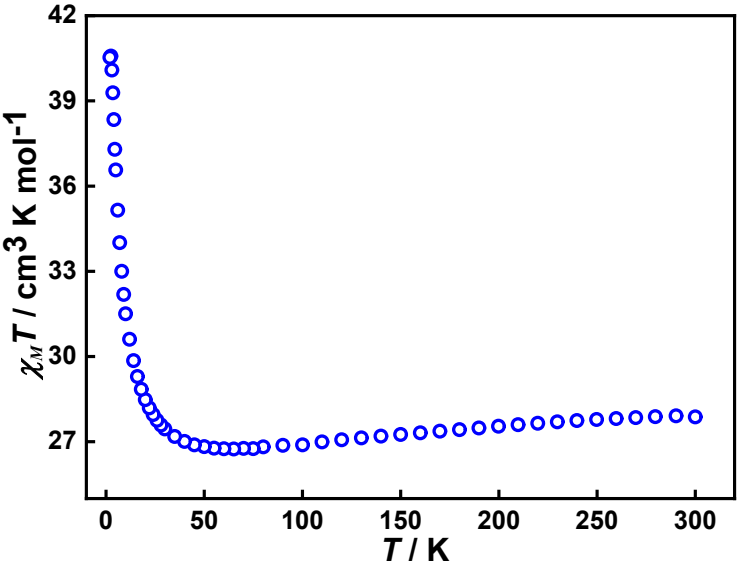

Figure S14. Plots of $\chi_M T$ versus T for **2S** in an applied magnetic field of 1 kOe. $\chi_M T$ (300 K) = 24.61 cm^3 K mol^{-1}, $\chi_M T$ (75 K) = 27.87 cm^3 K mol^{-1}, $\chi_M T$ (2 K) = 40.53 cm^3 K mol^{-1}.

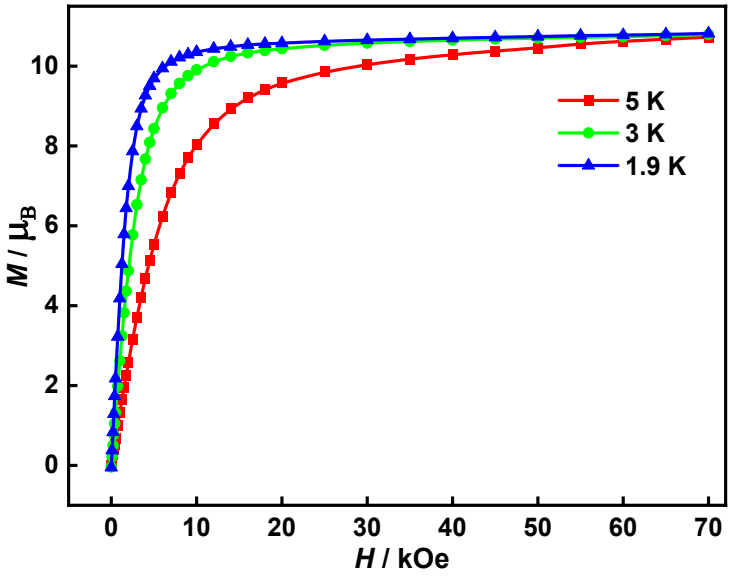

Figure S15. Field dependence of the magnetization at 1.9 K, 3 K and 5 K for **2S**. M = 10.82 μ_B at 1.9 K and 70 kOe.

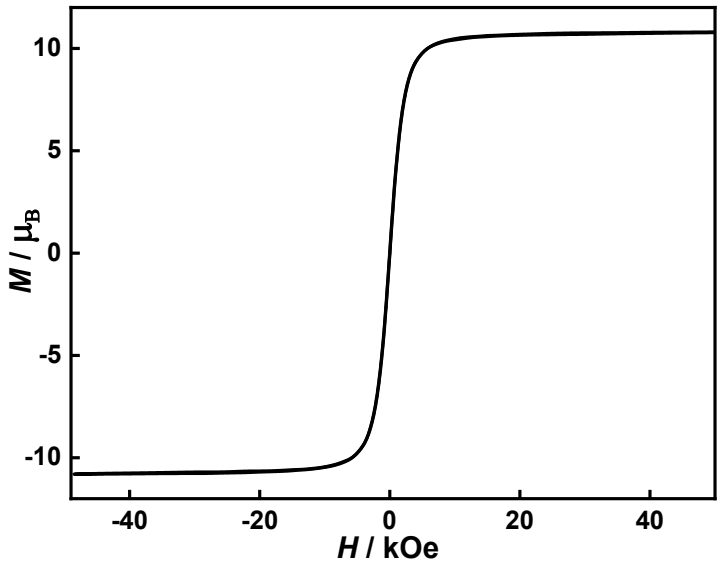

Figure S16. Magnetic hysteresis loop for **2S**. The data were collected at 1.9 K using an average field sweep speed of 31 Oe s^{-1}.

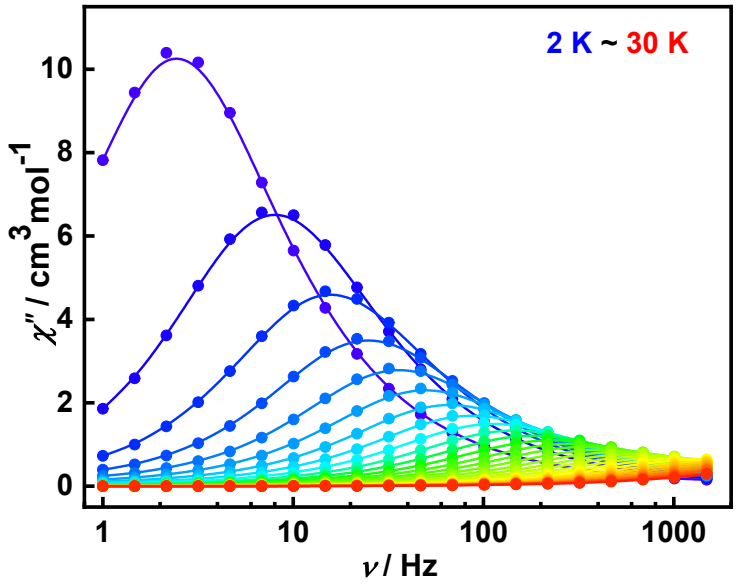

Figure S17. Frequency dependence of the out-of-phase susceptibility (χ'') for **2S** in zero DC field at AC frequencies of 1-1488 Hz in the temperature range of 2 to 30 K.

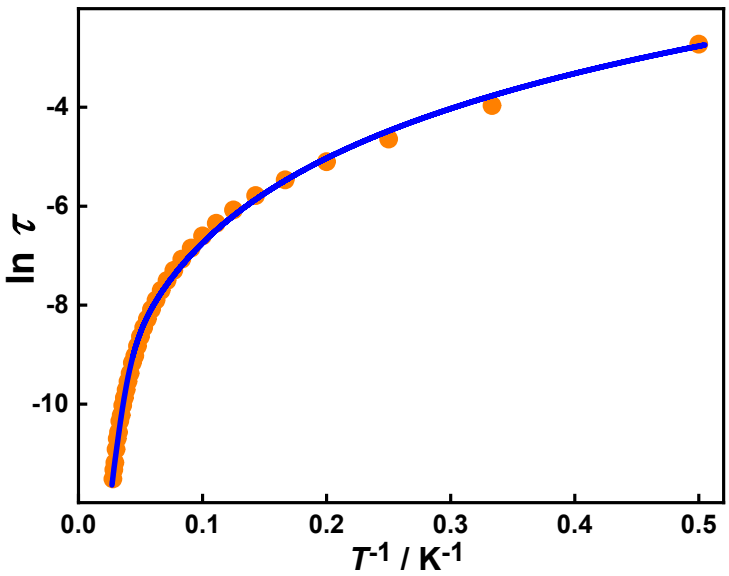

Figure S18. Temperature dependence of the relaxation time in the form of natural logarithm for **2S**. The blue line represents the fitting. The fitting equation is $\ln(\tau) = -\ln[CT^n + \tau_0^{-1}\exp(-U_{eff}/k_BT)]$, giving $U_{eff} = 160(13)$ cm^{-1}, $\tau_0 = 2.1(1) \times 10^{-8}$ s, $C = 2.9(2)$ s^{-1} K^{-n}, $n = 2.47(3)$.

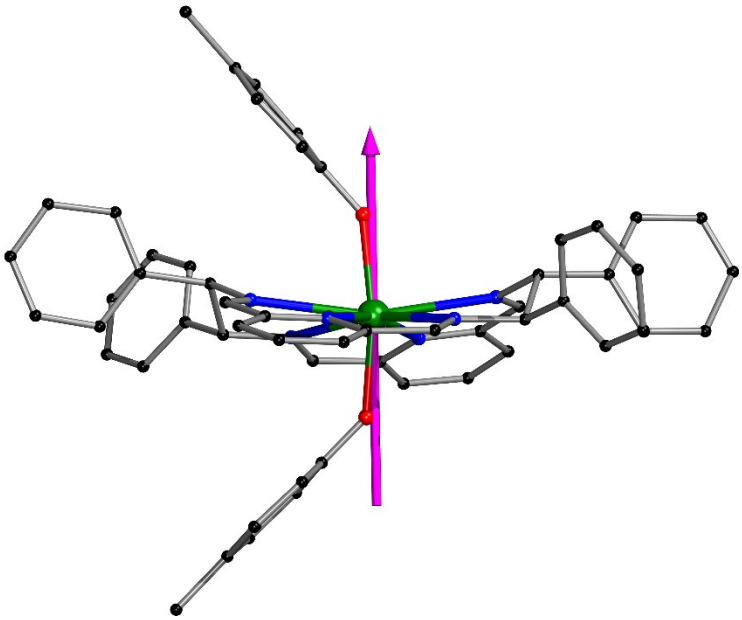

Figure S19. Ground-state magnetic anisotropy of complex **1R**. The pink line represents the orientation of the anisotropy axis for Dy^{III} ion.[3]

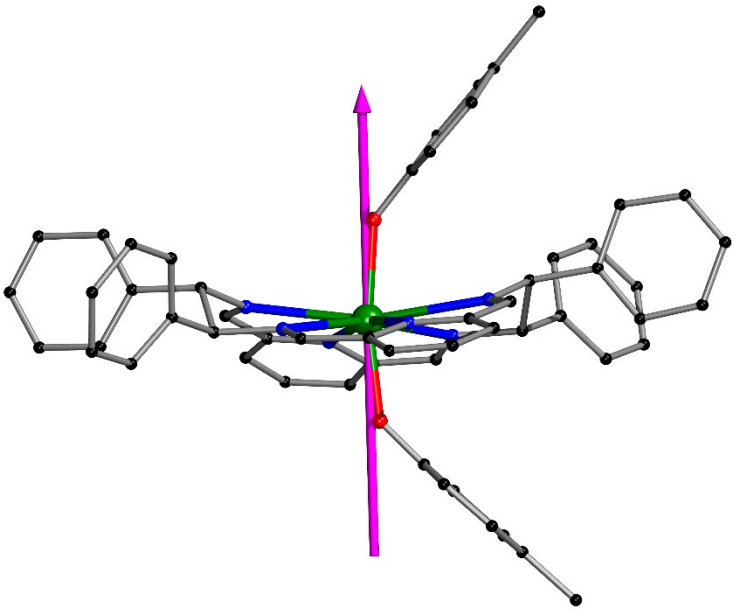

Figure S20. Ground-state magnetic anisotropy of complex **1S**. The pink line represents the orientation of the anisotropy axis for Dy^{III} ion.[3]

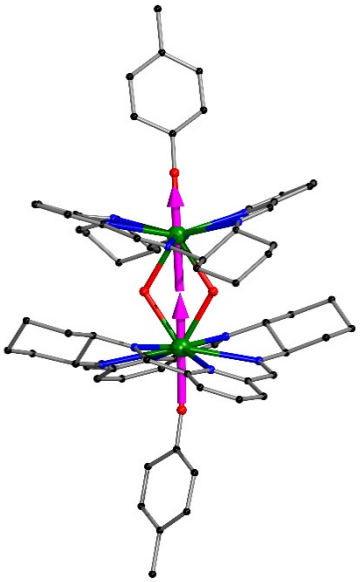

Figure S21. Ground-state magnetic anisotropy of complex **2R**. The pink lines represent the orientations of the anisotropy axes for Dy^{III} ions.[3]

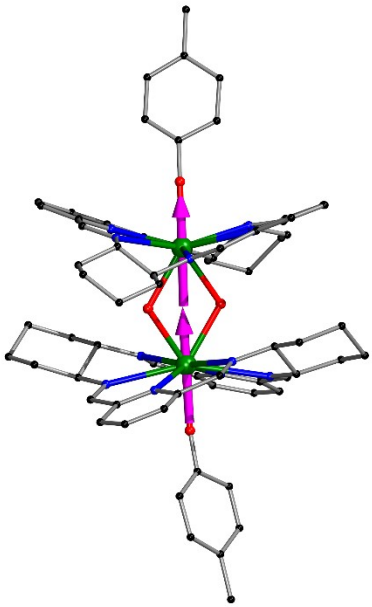

Figure S22. Ground-state magnetic anisotropy of complex **2S**. The pink lines represent the orientations of the anisotropy axes for Dy^{III} ions.[3]

Reference

1. M. Pinsky and D. Avnir, Continuous Symmetry Measures. 5. The Classical Polyhedra, *Inorg. Chem.*, 1998, **37**, 5575-5582.
2. D. Casanova, J. Cirera, M. Llunell, P. Alemany, D. Avnir and S. Alvarez, Minimal Distortion Pathways in Polyhedral Rearrangements, *J. Am. Chem. Soc.*, 2004, **126**, 1755-1763.
3. N. F. Chilton, D. Collison, E. J. L. McInnes, R. E. P. Winpenny and A. Soncini, An electrostatic model for the determination of magnetic anisotropy in dysprosium complexes, *Nat. Commun.*, 2013, **4**, 2551.